6-28-2008

Methane, Manganese, and Helium in Hydrothermal Plumes following Volcanic Eruptions on the East Pacific Rise near 9°500N

Brooke Love
Western Washington University, brooke.love@wwu.edu

Joseph A. (Joseph Anton) Resing
Pacific Marine Environmental Laboratories

James P. Cowen
University of Hawaii, Manoa

John E. Lupton
Pacific Marine Environmental Laboratories

Daniel J. Fornari
Woods Hole Oceanographic Institution

See next page for additional authors

Recommended Citation

Love, B. A., J. A. Resing, J. P. Cowen, J. E. Lupton, D. J. Fornari, T. M. Shank, and D. Biller (2008), Methane, manganese,and helium in hydrothermal plumes following volcanic eruptions on the East Pacific Rise near 9°500N, Geochem. Geophys.Geosyst., 9, Q06T01, doi:10.1029/2008GC002104.

Authors
Brooke Love, Joseph A. (Joseph Anton) Resing, James P. Cowen, John E. Lupton, Daniel J. Fornari, Timothy M. (Timothy Mitchell) Shank, and Dondra Biller

Geochemistry Geophysics Geosystems G3
AN ELECTRONIC JOURNAL OF THE EARTH SCIENCES
Published by AGU and the Geochemical Society

Article
Volume 9, Number 6
28 June 2008
Q06T01, doi:10.1029/2008GC002104
ISSN: 1525-2027

Methane, manganese, and helium in hydrothermal plumes following volcanic eruptions on the East Pacific Rise near 9°50′N

Brooke A. Love
School of Oceanography, University of Washington, Box 35531, Seattle, Washington 98195, USA (blove@ocean.washington.edu)

Joseph A. Resing
Pacific Marine Environmental Laboratory, National Oceanic and Atmospheric Administration, 7600 Sandpoint Way, Seattle, Washington 98115, USA

James P. Cowen
Department of Oceanography, School of Ocean and Earth Science and Technology, University of Hawaii at Manoa, Honolulu, Hawaii 96822, USA

John E. Lupton
Pacific Marine Environmental Laboratory, National Oceanic and Atmospheric Administration, Newport, Oregon 97365, USA

Daniel J. Fornari
Geology and Geophysics Department, Woods Hole Oceanographic Institution, Woods Hole, Massachusetts 02543, USA

Timothy M. Shank
Biology Department, Woods Hole Oceanographic Institution, Woods Hole, Massachusetts 02543, USA

Dondra Biller
Pacific Marine Environmental Laboratory, National Oceanic and Atmospheric Administration, 7600 Sandpoint Way, Seattle, Washington 98115, USA

[1] As part of a rapid response cruise in May 2006, we surveyed water column hydrothermal plumes and bottom conditions on the East Pacific Rise between 9°46.0′N and 9°57.6′N, where recent seafloor volcanic activity was suspected. Real-time measurements included temperature, light transmission, and salinity. Samples of the plume waters were analyzed for methane, manganese, helium concentrations, and the $\delta^{13}C$ of methane. These data allow us to examine the effects of the 2005–2006 volcanic eruption(s) on plume chemistry. Methane and manganese are sensitive tracers of hydrothermal plumes, and both were present in high concentrations. Methane reached 347 nM in upper plume samples (250 m above seafloor) and exceeded 1085 nM in a near-bottom sample. Mn reached 54 nM in the upper plume and 98 nM in near-bottom samples. The concentrations of methane and Mn were higher than measurements made after a volcanic eruption in the same area in 1991, but the ratio of CH_4/Mn, at 6.7, is slightly lower, though still well above the ratios measured in chronic plumes. High concentrations of methane in near-bottom samples were associated with areas of microbial mats and diffuse venting documented in seafloor imagery. The isotopic composition of the methane carbon shows evidence of active microbial oxidation; however, neither the fractionation factor nor the source of the eruption-associated methane can be determined with

any certainty. Considerable scatter in the isotopic data is due to diverse sources for the methane as well as fractionation as methane is consumed. One sample at +21‰ versus Peedee belemnite standard is among the most enriched methane carbon values reported in a hydrothermal plume to date.

Components: 8943 words, 6 figures, 2 tables.

Keywords: hydrothermal; plume; methane isotopes.

Index Terms: 1034 Geochemistry: Hydrothermal systems (0450, 3017, 3616, 4832, 8135, 8424); 1030 Geochemistry: Geochemical cycles (0330); 1041 Geochemistry: Stable isotope geochemistry (0454, 4870).

Received 19 May 2008; **Accepted** 23 May 2008; **Published** 28 June 2008.

Love, B. A., J. A. Resing, J. P. Cowen, J. E. Lupton, D. J. Fornari, T. M. Shank, and D. Biller (2008), Methane, manganese, and helium in hydrothermal plumes following volcanic eruptions on the East Pacific Rise near 9°50′N, *Geochem. Geophys. Geosyst.*, *9*, Q06T01, doi:10.1029/2008GC002104.

Theme: Recent Volcanic Eruptions, Properties, and Behavior of the Fast Spreading East Pacific Rise at 8°–11°N

1. Introduction

[2] A volcanic eruption near 9°50′N on the East Pacific Rise (EPR) (Figure 1) was discovered in April 2006 when several ocean bottom seismometers (OBSs) either did not respond to acoustic signals or responded but failed to release from their anchors during a National Science Foundation Ridge 2000 field program at the EPR integrated study site [*Tolstoy et al.*, 2006]. Subsequent water column measurements using miniature autonomous plume recorders (MAPRs) [*Baker and Milburn*, 1997] deployed from the research vessel (R/V) *Knorr* showed temperature and turbidity anomalies indicative of a possible eruption. An R/V *New Horizon* rapid response cruise (NH-06) in May 2006, was staged within a week of the discovery and confirmed the recent volcanic eruptions. Preliminary results from that cruise are presented by *Cowen et al.* [2007], and results from mapping the new eruptions are presented by *Soule et al.* [2007]. Radiometric ^{210}Po-^{210}Pb dating of fresh lavas collected from the new flows shows a range in age from summer 2005 through fall 2006 [*Rubin et al.*, 2006], while microseismic data show a 2-year ramp-up of earthquake activity that abruptly stopped in January of 2006, with large pulses throughout the summer and into late 2005 [*Tolstoy et al.*, 2006]. Detailed mapping of the new flows shows that the 2005–2006 eruption was large for this segment [*Soule et al.*, 2007].

[3] Methane and Mn concentrations are sensitive indicators of hydrothermal activity, and have been used in previous studies on the effects of seafloor volcanic eruptions on plume chemistry [e.g., *Cowen et al.*, 1998; *Lupton et al.*, 1993; *Mottl et al.*, 1995], and microbial methane oxidation [e.g., *Cowen et al.*, 2002; *de Angelis et al.*, 1993; *Gharib et al.*, 2005; *Kadko et al.*, 1990]. Two studies on post-eruption plumes at Gorda Ridge and Axial Volcano [*Kelley et al.*, 1998; *McLaughlin-West et al.*, 1999] were extremely different in terms of methane concentration and ratios to other constituents (Table 1). At Gorda, methane was only slightly elevated above background one to four months following the volcanic event in both the event plume and perturbed chronic plumes. $CH_4/^3He$ and CH_4/Mn were also relatively low at Gorda though $CH_4/^3He$ was slightly elevated in the event plume [*Kelley et al.*, 1998]. At Axial, one month following the eruption, methane, $CH_4/^3He$ and CH_4/Mn were all much higher than values measured at Gorda. In addition, methane stable isotopic composition was determined to be quite uniform, with an average of −32.7‰ ± 0.8 for samples with methane concentration greater than 10 nM [*McLaughlin-West et al.*, 1999]. *McLaughlin-West et al.* [1999] were unable to determine whether the source of the event-related methane at Axial was the breakdown of organic matter or microbial production, and there was no evidence of microbial oxidation of methane in the plume. It is unclear why the event at Gorda Ridge did not appear to generate appreciable event-related methane while the Axial event did.

[4] The EPR event is the first documented repeat eruption at a single site on the mid-ocean ridge

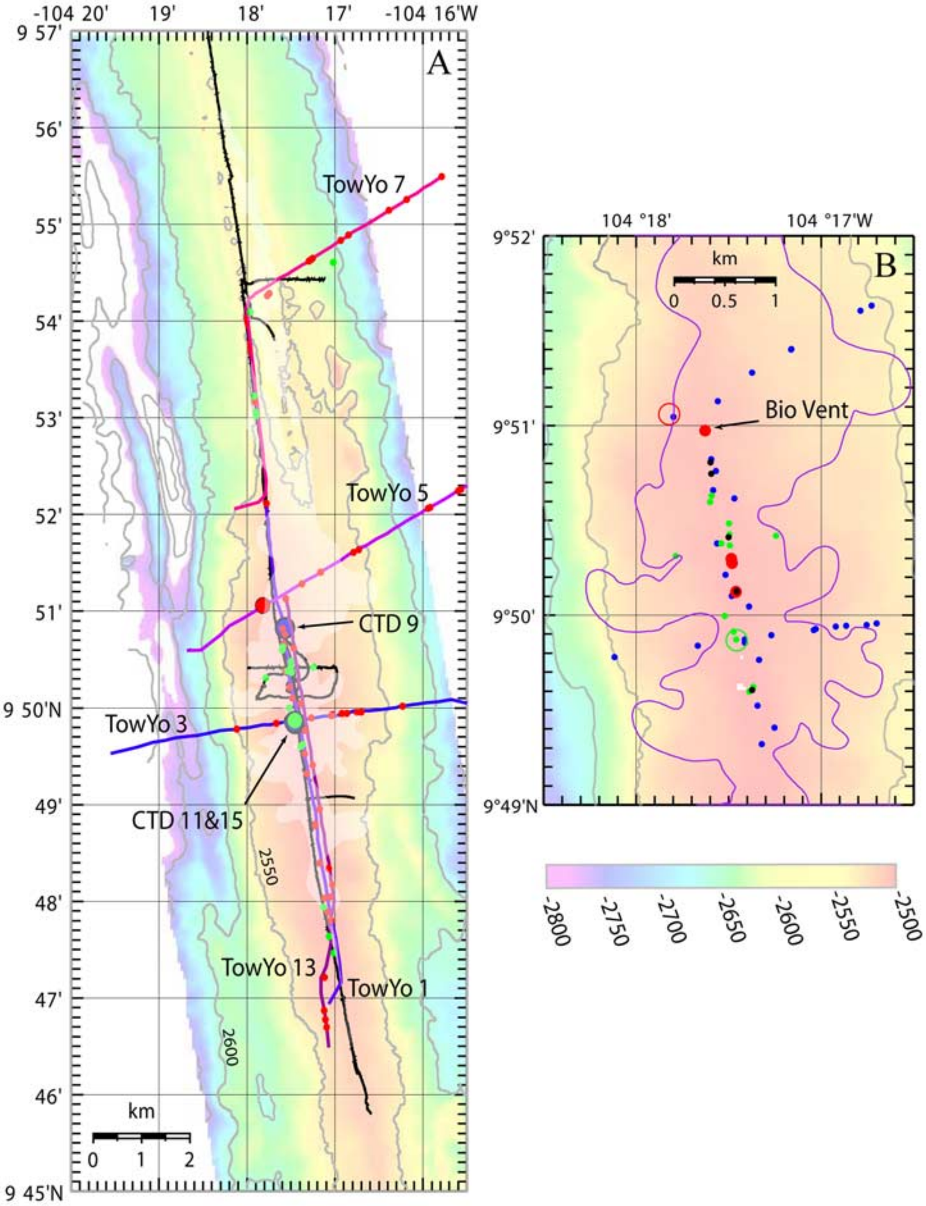

Figure 1. Figure 1a is a map showing tow paths of CTD tow-yos (solid lines), TowCam tracks (black), position of tow-yo bottles (red) and TowCam bottles (green), and two vertical casts (blue). Bathymetry is from *White et al.* [2006] with the depth scale given on the color bar, with the transparent layer delineating the extent of the most recent lava flows [*Soule et al.*, 2007]. The larger red point is the location of the +21% δ^{13}C sample (NW of "BioVent" high-temperature vent), and the larger green point is the location of the TowCam image in Figure 3 that corresponds to elevated near-bottom methane. Figure 1b shows the locations of high-temperature vent in red, extinct vents in black, TowCam samples in green, and upper plume samples in blue. The open red circle is the +21% δ^{13}C sample, and the open green circle is the location of the TowCam image shown in Figure 3, while the extent of fresh lava flows is shown in purple.

(MOR), and this area has been the subject of intensive study since a volcanic eruption was documented there in 1991 [*Haymon et al.*, 1993; *Rubin et al.*, 1994]. Geological, chemical and ecosystem characteristics of this fast spreading MOR have been the focus of numerous studies, which provide an excellent baseline for changes related to the latest eruption [e.g., *Escartín et al.*, 2007; *Ferrini et al.*, 2007; *Fornari et al.*, 1998a, 1998b, 2004; *Lilley et al.*, 1991; *Lutz et al.*, 1994; *Mottl et al.*, 1995; *Shank et al.*, 1998; *Von Damm*, 2000; *Von Damm et al.*, 1995]. A study of the plume chemistry seven months after the 1991 event showed elevated methane concentrations, manga-

Table 1. Summary of Eruption-Related Methane and Manganese Plume Data

	Max. CH_4 (nM)	$CH_4/^3He \times 10^6$	CH_4/Mn	Max. Mn (nM)	$\delta^{13}C$-CH_4 (‰)	Comments
Gorda 1996[a]						1–4 months after event
Chronic	7	1	0.05			
Event	5	2–3	0.1			
Axial Volcano[b]	522	17–37	2.2 average		−32.7 ± 0.8	1 month after event
This site 1991[c]						Approx. 7 months after event(s)
Eruption area	89	6	10.5	18		
Adjacent areas	35	0.5	1.5	37		
North Segment	6		0.08	78		
This site 2006						4–9 months after event(s)
Upper plume mean	347		6.6	55		
Std. dev.	81 ± 63	13.5 ± 0.9	2.3 ± 1.4	34 ± 9	−19.2 ± 9.5	
This site 2006						4–9 months after event(s)
Near-bottom mean	1085		4.4	98.1		
Std. dev.	218 ± 327	12.5 ± 0.7	2.6 ± 1.6	42 ± 26	−30.3 ± 6.8	

[a] *Kelley et al.* [1998].
[b] *McLaughlin-West et al.* [1999].
[c] *Lupton et al.* [1993]; *Mottl et al.* [1995].

nese concentrations, and CH_4/Mn ratios in the immediate area of the eruption [*Mottl et al.*, 1995] (Table 1). The chemistry of the plumes overlying the 1991 site was notably chaotic, with markedly poor correlations between parameters that are normally closely related in stable chronic plumes. $CH_4/^3He$ on this segment was also elevated relative to the northern segment (north of the Clipperton Transform Fault) which was not effected by the 1991 event [*Lupton et al.*, 1993] (Table 1).

[5] Here we present methane, Mn, and helium-3 concentrations, and stable isotopic composition of the methane carbon from plume samples collected during the R/V *New Horizon* cruise (NH06) in May 2006. Given the various estimates for the timing of the extrusive events [*Cowen et al.*, 2007; *Rubin et al.*, 2006; *Tolstoy et al.*, 2006] it is likely that 4–9 months elapsed between eruption of new lava flows and collection of these samples. The residence time of methane in hydrothermal plumes is on the order of 7 to 11 days [*de Angelis et al.*, 1993; *Kadko et al.*, 1990], therefore the samples can be assumed to represent fluids evolving from the seafloor at the time of sampling or shortly preceding it. We examine the effects of the 2005/6 volcanic eruption(s) on plume chemistry and compare them to plume observations following other volcanic events, specifically the 1991/1992 eruptions at this site. Measurements of the carbon isotopic composition of methane show evidence of microbial methane oxidation in the plume and place the least diluted samples in the range of the isotopic composition of known sources of hydrothermal methane at this site.

2. Study Site

[6] The EPR south of the Clipperton Transform Fault is a fast spreading ridge, with a full spreading rate of 11 cm/a [*Carbotte and Macdonald*, 1992]. It exhibits an apparently high magmatic budget as indicated by the relatively shallow topography of the ridge crest, a distinct axial summit trough, and a rectangular cross section along most of its length [e.g., *Fornari et al.*, 1998a; *Macdonald et al.*, 1992; *Scheirer and Macdonald*, 1993]. A seismic reflector 1.2 to 2 km below the seafloor is interpreted as the top of the axial magma body [*Detrick et al.*, 1987; *Kent et al.*, 1993]. Extensive areas of both high-temperature and low-temperature venting have been documented, as well as the associated biological communities [*Fornari et al.*, 1998b; *Shank et al.*, 1998; *Von Damm*, 2000; *Von Damm et al.*, 1995]. Tow-yo and TowCam tracks in this study cover many of these areas, which are likely to continue to be sites of active hydrothermal activity, similar to what was observed following the 1991 EPR eruption [e.g., *Ferrini et al.*, 2007; *Fornari et al.*, 2004; *Shank et al.*, 1998; *Von Damm and Lilley*, 2004].

3. Methods

[7] Shipboard equipment included a conductivity temperature depth (CTD) package with 10 L Nis-

kin-style water sampling bottles, a SeaTech light scattering sensor (LSS), Wetlabs Transmissometer, ISEA Electrochemical Analyzer, and a SeaBird high-precision CTD system for temperature, salinity and pressure. Three along-axis tow-yos (in which the package is towed in a saw tooth pattern through the lower several hundred meters of the water column), three cross-axis tow-yos and two vertical casts were carried out with the CTD package. A towed deep-sea camera system [*Fornari*, 2003; *Soule et al.*, 2007], including a digital camera, rock sampling capabilities, four 5-L Niskin bottles, a SeaBird-25 CTD system, and Sea Tech LSS was also deployed for seven near-bottom tows, primarily along the EPR axis (Figure 1). During each lowering, the TowCam was towed ~4 to 6 m above the seafloor at ~0.25 to 0.5 knots for ~5 h. The Tow Cam acquired an image every 10 s, which resulted in subject plane overlap in consecutive images in approximately 70% of the ~1800 images collected during each tow. Hydrothermal activity, as observed by TowCam, extended from 9°46.5′N to 9°54.9′N [*Cowen et al.*, 2007]. TowCam Niskin samples were collected within the most spatially concentrated area of venting (less than tens of meters spacing), which was between 9°49.7′N and 9°51.5′N (Figure 1). Microbial-like material existed in all areas of active venting in which TowCam Niskin samples were recovered. Of the 22 Niskin samples obtained using TowCam, eight were collected near areas with white microbial mat material indicative of active diffuse flow venting. Additionally, eight near-bottom samples were taken adjacent to diffuse flow areas stained with iron oxy-hydroxide precipitate, and six samples were taken out of sight of the bottom. Images acquired during the collection of these six samples show the visibility was obscured due to flocculent ‘‘debris’’ in the water column. These samples are therefore considered to be proximal to diffuse flow sites.

[8] Subsamples for gas measurements were taken from the Niskins immediately upon recovery. Samples for methane concentration were drawn into 140 mL syringes and analyzed on board via a helium headspace technique on a portable gas chromatograph within hours of sampling, similar to that described by *Kelley et al.* [1998]. Detection limit for methane is 0.3 nM, and precision is ±5%. Samples for methane δ^{13}C composition were drawn with no headspace into combusted 200 mL glass serum bottles, preserved with 750 μL of saturated $HgCl_2$ solution and closed with butyl rubber stoppers and aluminum crimp seals. Shore-based analysis was carried out on a Finnigan MAT252 mass spectrometer with GC1 interface similar to *Popp et al.* [1995] and *Sansone et al.* [1997], with a precision of less than 0.8‰ for replicate samples. For collection of He samples, copper tubing was flushed with sample water and press-sealed using bolted clamps for later laboratory extraction and analysis by isotope ratio mass spectrometry, similar to *Kelley et al.* [1998]. Total dissolvable manganese samples were collected in acid washed 250 mL polyethylene bottles and acidified with 1 mL of 6 N subboiling, distilled hydrochloric acid. Samples were stored and analyzed by a newly developed method based on sequential injection analysis with spectrophotometric detection, which allows the use of small volumes of sample and reagents by mixing in line, where the sample mixing volume is contained between air bubbles in small diameter tubing (D. Biller et al., manuscript in preparation, 2008). Precision of the manganese measurement was ±4% with a limit of detection of ~1.5 nM.

[9] Potential temperature (θ) and potential density (σ_θ) were calculated on the basis of pressure, temperature and salinity measured in situ, according to *Jackett et al.* [2006]. Potential temperature anomalies ($\Delta\theta$) were calculated according to equation (1) of *Baker et al.* [1994].

4. Results

[10] During seven days on station, three tow-yos and three camera tows were performed along the ridge axis between 9°46′N and 9°57.6′N. In addition, three tow-yos and three camera tows were performed in cross-axis orientations at several points along the EPR axis. Two vertical CTD casts and one vertical TowCam cast were also carried out (Figure 1). The most intense particle plumes were centered over 9°46.6′N and 9°51.5′N and advection of plumes was primarily to the east of the axis during the cruise.

[11] Density inversion layers were found throughout the deepest 250 m of water between 9°48.5′N and 9°50.5′N, which made the calculation of accurate potential temperature anomalies problematic. Errors estimated for this calculation are on the same order as the anomalies themselves (at least ±0.001°C) in the upper plume. This instability in the water column is consistent with vigorous hydrothermal venting and indicates the presence of a buoyant plume. The strongest density inversions occur in the same areas as the highest estimated temperature anomalies (0.002 to >0.008°C)

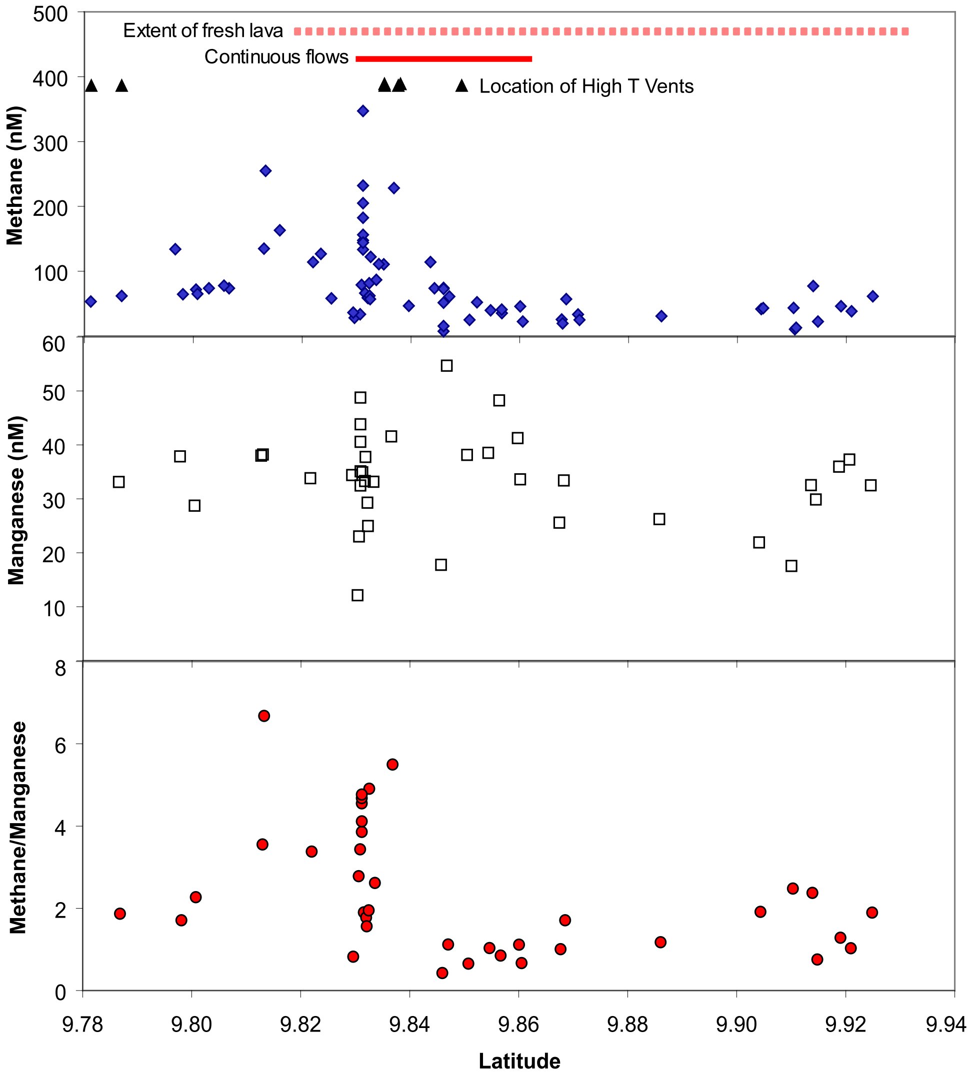

Figure 2. Upper plume methane, manganese, and CH_4/Mn versus latitude. The dotted line indicates the extent of fresh flows. The solid line indicates the extent of the area of the most continuous flows. Maximum values for all three parameters were measured near the area of most continuous flows.

[*Cowen et al.*, 2007; *Tolstoy et al.*, 2006]. Small temperature anomalies were also calculated following the 1991 event and were attributed to hydrographic masking of $\Delta\theta$ due to the low salinity of the hydrothermal fluids [*Lupton et al.*, 1993].

4.1. Manganese Abundance

[12] Total dissolvable manganese concentrations were measured on 47 samples from plume and near-bottom depths (Figure 2 and Data Set S1[1]). The maximum concentration and average values for samples collected with the CTD rosette, between 10 m and 300 m above the seafloor (upper plume samples) was smaller than that in samples collected with the TowCam bottles 2 m to 8 m above the seafloor (near-bottom samples) (Table 1). In cast 9, the most complete vertical profile in the upper plume, manganese reaches a maximum at 115 m above bottom, the same depth as a local maximum in methane.

4.2. Methane Abundance

[13] Elevated methane concentrations to 347 nM were measured in upper plume samples collected from the CTD rosette system while background concentrations were 0.5 to 0.9 nM. The mean value for methane concentration in upper plume samples was 81 nM with a standard deviation of 63, while the mean in near-bottom samples was 218 nM with

---

[1] Auxiliary materials are available at ftp://ftp.agu.org/apend/gc/2008gc002104.

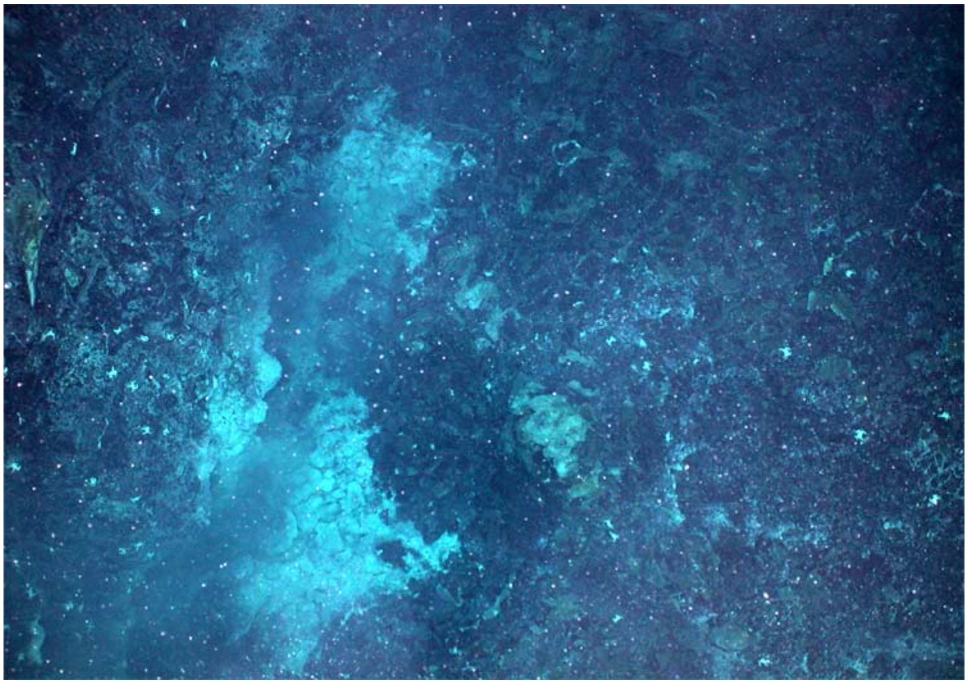

Figure 3. Digital TowCam image of posteruptive diffuse flow emanating from a microbially lined fissure below the margin of a collapse terrace in the margin of the axial summit trough of the East Pacific Rise (see Figure 1 for location). This seafloor location corresponds to the collection of Niskin fluids (Tow 15, bottle 7) from which one of the highest methane concentrations (1085 nM) was observed (seafloor depth 2493 m; altitude 2.4 m; scale across bottom of image = ~3 m).

a standard deviation of 327 nM. Methane levels to 1085 nM were measured in near-bottom samples collected during TowCam surveys (Table 1 and Data Set S1).

4.3. Methane Carbon Isotopic Composition

[14] Measured δ^{13}C values in this study range from −43.8‰ versus a Peedee belemnite standard (PDB) in a background sample, to +21.5‰, in a sample obtained just NW of the BioVent high-temperature vent (Cast 5, bottle 2; see Figure 1 for location). This +21.5‰ sample is one of the most isotopically enriched methane carbon values reported in a hydrothermal plume to date, compared to enriched values of +11‰ reported at Endeavor and +40.4‰ in the southern Okinawa Trough [*Cowen et al.*, 2002; *Gamo et al.*, 2003]. Near-bottom samples were, on average, significantly more depleted than upper plume samples (Table 1 and Data Set S1).

4.4. TowCam

[15] TowCam surveys covered many areas that had been densely populated by mussel beds and tube worms which had colonized the area over the 15 year interval since the last eruption [e.g., *Shank et al.*, 1998]. Most of these established vent communities appear to have been covered by the fresh flows. Very active diffuse-flow venting was imaged by TowCam (Figure 3), and was characterized by increased temperature, milky fluids or fluids bearing white flocculent material, and extensive white microbial mats covering glassy new flows. Areas characterized by olive brown colored mats were also imaged. These areas did not have obvious active flow, and these mats may represent remnants of the white mats after fluid flow has slowed or stopped. Because the lag between triggering and closing of the bottle is 12–15 s (or ~3 m), near-bottom Niskin samples were most often collected when the TowCam CTD measured increases of 0.5°C that persisted for one to three minutes. This procedure ensured that water samples were generally still within the area of anomalously high temperature; however, spatial heterogeneity near the seafloor may decouple the chemistry of Niskin samples (e.g., methane, Mn) from the sensor parameters (e.g., θ, salinity) to some extent. The samples that showed extremely high methane concentrations were typically collected near areas of both white microbial mats, and diffuse flow issuing from fissures.

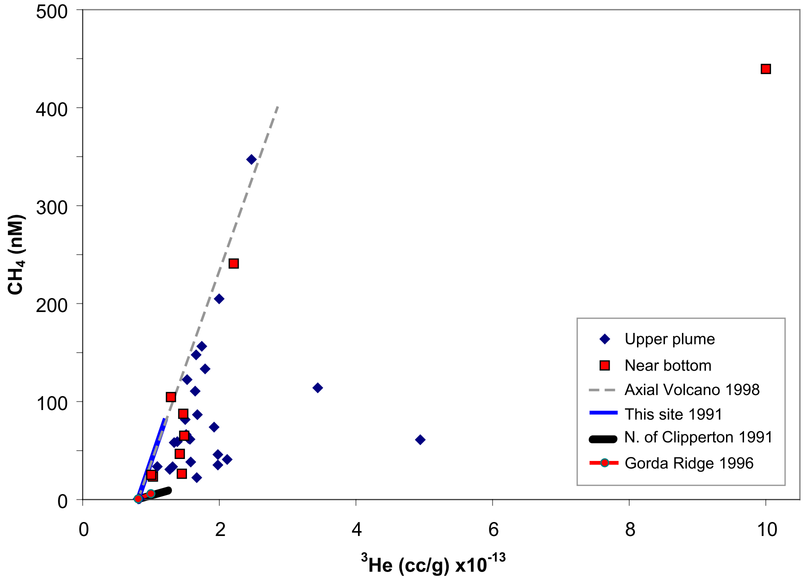

Figure 4. Methane versus ^{3}He. These data demonstrate the variability of methane to ^{3}He in source fluids and effects of dilution and oxidation. Trends from previous studies are included for comparison, including this site and the area north of the Clipperton Transform fault in 1991 [*Lupton et al.*, 1993; *Mottl et al.*, 1995], Gorda Ridge [*Kelley et al.*, 1998], and Axial Volcano [*McLaughlin-West et al.*, 1999].

4.5. Helium-3

[16] Helium-3 was measured in nine near-bottom samples and 28 upper plume samples, including four background samples. Background concentrations for ^{3}He averaged $8.21 \times 10^{-14} \pm 0.12 \times 10^{-14}$ cc/g. ^{3}He measured in upper plume samples was less abundant and less variable than in near-bottom samples (Table 1 and Data Set S1). The mean and range of $CH_4/^3He$ was similar in both the near-bottom and the upper plume samples (Table 1 and Figure 4). Mn and ^{3}He were correlated in upper plume samples (R = 0.74).

5. Discussion

5.1. Manganese Abundance

[17] The maximum upper plume Mn concentration of 55 nM measured in this study is somewhat higher than, but comparable to data from the previous eruption at this site. Along this segment, Mn reached only 37 nM in 1991, and less than 20 nM in the immediate vicinity of the eruption [*Mottl et al.*, 1995]. The average value of 34 nM total dissolvable Mn in the upper plume is slightly higher than the average in 1991, possibly due to the influence of highly vapor dominated fluids postulated in the formation of the plumes in the immediate vicinity of the 1991 eruption.

[18] Methane and Mn in upper plume samples both reach their maximum concentrations near active high-temperature vents (T. Shank and K. Von Damm, personal communication, 2007) and continuous new lava flows [*Soule et al.*, 2007] (Figures 1 and 2). The range of Mn concentrations measured in this study is similar to the range in the areas directly adjacent to the area of the 1991 eruption [*Mottl et al.*, 1995]. Such similarity suggests that a consistent set of processes influence plume chemistry following magmatic events at this site.

5.2. Methane Abundance

[19] Methane concentrations measured in this study are 4 to 100 times higher than those normally associated with chronic plumes overlying unsedimented hydrothermal systems [*Lilley et al.*, 1995]. The upper plume maximum of 347 nM is larger than the maximum methane concentrations of 89 nM recorded in the plume 7 months after the 1991 eruption [*Mottl et al.*, 1995].

[20] The higher mean values for methane concentration in the near-bottom samples compared to upper plume samples (Table 1) may indicate that near-bottom samples are more influenced by low-temperature venting. Diffuse fluids often have higher methane concentrations than high-temperature venting and are more likely to be influenced by methanogens [*Lilley et al.*, 1991; *Proskurowski*

et al., 2008]. This difference could also be explained by the higher degree of entrainment of low-methane water in the upper plume.

[21] Studies that have observed increased methane in hydrothermal fluids in association with shallow intrusion of lava have not attributed that increase to a specific source [e.g., *McLaughlin-West et al.*, 1999; *Mottl et al.*, 1995]. In general, hydrothermal methane in basalt-hosted systems derives from several distinct sources: (1) out-gassed juvenile methane from the mantle dissolved directly into hydrothermal fluids or extracted from fluid inclusions and grain boundaries in basalts; (2) equilibrium with CO_2 and H_2 at high temperatures, generally at temperatures greater than 500°C; (3) thermal breakdown of organic matter and hydrocarbons (thermogenic); and (4) microbial production at low to moderate temperatures [*Welhan*, 1988]. Distinctions between these sources are often made on the basis of the isotopic composition of the methane. The first two sources are difficult to distinguish in practice and can be referred to jointly as high-temperature methane. All of these processes are possible sources of the methane in the fluids we sampled. The formation of methane during the serpentinization of ultramafic rocks is probably not important at the EPR because the extent of faulting and hydrothermal circulation is believed to lie mainly above a relatively shallow crustal magma lens where fluids would not interact with peridotites [e.g., *Tolstoy et al.*, 2008]. In addition, none of the numerous studies of basalt geochemistry and morphology on the EPR have reported ultramafic rocks exposed on the seafloor [e.g., *Langmuir et al.*, 1986; *Perfit and Chadwick*, 1998; *Perfit et al.*, 1994].

5.3. Methane/Helium-3

[22] Methane is plotted versus ^{3}He in Figure 4. Neither the near-bottom nor the upper plume data in this study fall along a simple trend or dilution line. This is probably due to a combination of two factors. First, there is likely some variation in the ratio of methane to ^{3}He in the source fluids because methane is produced through processes not directly linked to magma degassing. Second, as the plume ages, methane is consumed by microbial activity while helium is not, which results in a decrease in the ratio of methane to ^{3}He. The range of ratios measured here falls within the range of those previously measured in post-eruption plumes. The largest ratios observed here are similar to those found in post-eruption plumes at this site in 1991 and at Axial volcano in 1998, while the lowest ratios are similar to those following the Gorda event and at the EPR North of the Clipperton transform fault. These lower ratios appear to be close to a lower limit, where little additional methane is observed, while the upper limit demonstrates that excess methane is commonly associated with recent eruptions.

5.4. Methane/Manganese

[23] The correlation coefficient for methane and Mn in upper plume samples is 0.44 for 39 samples. A similarly poor correlation was observed in this area in 1991, in contrast to correlation coefficients greater than 0.95 on >100 samples measured in 1991 north of the Clipperton Transform Fault [*Mottl et al.*, 1995]. A decoupling of methane and Mn would be expected if fluids were effectively segregated into vapor- and brine-rich phases following phase separation. Alternatively, this decoupling of methane and Mn would be expected if the primary source of methane is the thermal breakdown of buried biological communities or methanogenesis. The production of methane by these processes would not correlate with the Mn emitted from high-temperature and low-temperature vents, regardless of phase separation processes. In addition, loss of methane as the plume ages will diminish the correlation of methane to Mn.

[24] Methane to manganese ratios from this study (up to a maximum value of 6.7) are greatly elevated relative to those typically associated with chronic plumes (0.02–0.1) [*Charlou et al.*, 1991; *Lilley et al.*, 1995; *Mottl et al.*, 1995 and references therein], but somewhat lower than the maximum values close to 10 measured after the 1991 eruption [*Mottl et al.*, 1995]. In this study, the highest methane and CH_4/Mn values were measured in the area in which the most continuous fresh lava flows were observed (9°48′N to 9°50′N; Figure 2). The ratio of CH_4/Mn is largely controlled by the methane concentration in this data set, as seen in the high correlation between methane and CH_4/Mn (correlation coefficient 0.94) and lack of significant correlation between Mn and CH_4/Mn. The variability of CH_4/Mn and its dependence on methane concentration can also be seen in a plot of methane versus Mn (Figure 5). The CH_4/Mn ratios in the area of the 1991 eruption were much higher (3–10) than those in adjacent areas (<2). Ratios were even lower (<0.1) north of the Clipperton Transform Fault between 10°20′ and 11°40′ (Figure 5) [*Mottl et al.*, 1995]. The high ratios in 1991 were a result

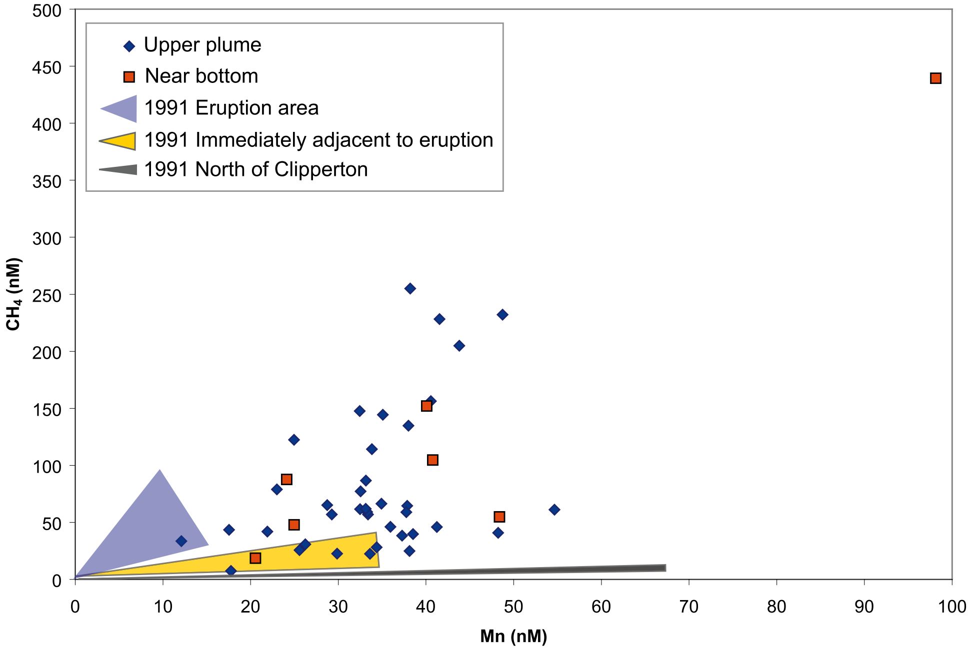

Figure 5. Manganese versus methane for samples from the upper plume (blue) and near bottom (red). Shaded areas indicate the range of methane to Mn ratios measured in 1991 in the eruption area (blue) the immediately adjacent areas (yellow) and the segment to the north of the Clipperton transform fault (gray) [*Mottl et al.*, 1995].

of both high methane, and low Mn concentrations, with Mn increasing as the ratio decreases. In contrast, our samples with high CH_4/Mn ratios have high methane concentrations, but a similar range of Mn concentrations to that of low ratio samples. This is consistent with microbial and/or thermogenic production of methane as the primary cause of the decoupling of methane and Mn in 2006. If phase separation is the dominant process, Mn concentration would tend to decrease in areas where methane increases, as was seen in the high ratio samples in 1991. A secondary role for phase separation in 2006 is also supported by the relatively good correlation between Mn and ^{3}He.

[25] An additional factor in the variability of CH_4/Mn is that low CH_4/Mn samples may represent older plume water from which the methane has been removed by microbial methane consumption. This is supported by the fact that all samples collected in plumes not directly above the ridge axis had $CH_4/Mn < 3$, with a single exception, while those samples collected on axis show a full range of CH_4/Mn values. This suggests that the off axis plume must have aged somewhat relative to those directly on axis. Off axis samples are also on average more enriched than on axis samples, as would be expected as they age.

5.5. Other Ratios and Correlations

[26] In unperturbed chronic plumes like the northern segment of the 1991 EPR study, hydrothermal parameters like methane, Mn, $\Delta\theta$, and light attenuation, are closely coupled [*Mottl et al.*, 1995]. These relationships are disrupted following magmatic events. In 1991 the samples near the newly erupted area, light attenuation correlated only with methane. In this study, light attenuation did not correlate well with any other measured parameter (i.e., no correlation coefficients greater than 0.5). In both studies, methane is largely decoupled from both Mn and potential temperature anomaly (Figures 5 and 6).

[27] Although methane is highly correlated with both Mn and ^{3}He in near-bottom samples (coefficients of 0.93 and 0.88 respectively), these correlations include less than ten samples on which each parameter was measured. This could indicate less variability in age and microbial consumption of methane and/or greater homogeneity in source fluids for these samples than for the upper plume samples but the scarcity of data weakens this interpretation significantly.

[28] Figure 6 shows the relationship between methane and potential temperature anomaly for both TowCam and upper plume samples. Overall, the

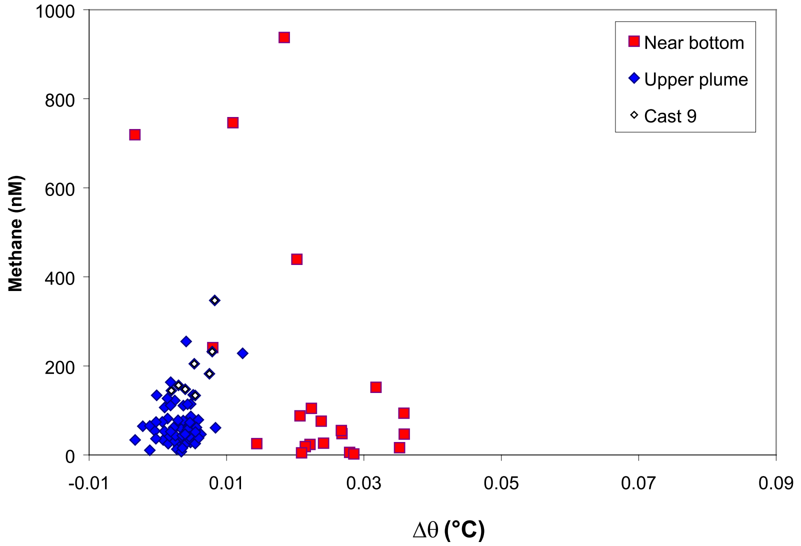

Figure 6. Methane concentration versus potential temperature anomaly ($\Delta\theta$) for plume depth and near-bottom samples. Some of the near-bottom samples with extremely high methane concentrations were collected in locations where the potential temperature was also very high (0.2 to 0.5°C higher than the surrounding areas). There is no strong relationship between methane and $\Delta\theta$ in either the upper plume or the near-bottom samples, though $\Delta\theta$ is higher in near-bottom samples than in the upper plume.

relationships of methane to potential temperature and potential temperature anomaly are very weak in both upper plume and near-bottom samples. Both the range and the average of the calculated potential temperature anomalies are higher in the near-bottom samples where entrainment of seawater is presumably less of a factor and there is less hydrographic masking of the signal. These upper plume results are similar to a study between 11°40′ and 13°N on the EPR, which found that temperature anomalies were not well correlated with chemical tracers and concluded that the complexity of the temperature profiles is indicative of hydrothermal activity but that further interpretation is difficult [*Charlou et al.*, 1991].

5.6. Fractionation of Methane

[29] As methane in plumes is consumed, the carbon isotopes fractionate, and the lighter (depleted) carbon is preferentially oxidized leaving the remaining methane heavier or more enriched in ^{13}C, yielding a more positive value for δ^{13}C [e.g., *Coleman et al.*, 1981; *Silverman and Oyama*, 1968]. The extremely large range in isotopic composition observed in this study (−43.8‰ to +21.5‰), points to an active oxidation process and a range of sources. The most concentrated sample in the upper plume was 347 nM, with δ^{13}C = −32.2‰, while near-bottom samples reached 1085 nM methane and δ^{13}C in these samples ranged from −30‰ to −37‰. The most depleted samples in this study were the background seawater with compositions between −41‰ to −43‰. The most ^{13}C enriched samples in this study are much more enriched than any samples previously collected at this site [*Proskurowski et al.*, 2008] (Table 2). This is almost certainly due to the enrichment of the residual methane after significant microbial oxidation which preferentially uses the lighter (more depleted) methane [e.g., *Cowen et al.*, 2002; *Gamo et al.*, 2003; *Sansone et al.*, 1999].

[30] The fractionation factor for methane oxidation in plumes can be estimated using the Rayleigh distillation technique; however, in order to do this, the fraction of the original methane remaining must be calculated using a conservative tracer (Mn or ^{3}He) to estimate dilution. In order for this calculation to be valid, the source fluids must have a constant ratio of methane to the tracer. *Charlou et al.* [1991] found that the $CH_4/^3He$ correlation in zero age plumes on the EPR was quite variable due to a vertical background gradient in ^{3}He, methane removal, and differences in source fluids, while CH_4/Mn in these plumes was relatively constant [*Charlou et al.*, 1991]. Neither Mn nor ^{3}He appear to be well correlated with methane in source fluids in our data set.

Table 2. Previously Reported Methane Isotopic Values From Vents at This Site[a]

	CH_4 (mmol/kg) Low T	CH_4 (mmol/kg) High T	$\delta^{13}C$-CH_4 Low T (‰)	$\delta^{13}C$-CH_4 High T (‰)	$\delta^{13}C$-CO_2(‰)
1991 Bio 9 Area	0.12	0.16	−26.8	−34.6	−3.8 to −5.4
1995–1997 Bio 9 Area	0.06	0.09	−25.2 to −26.2	−18.9 to −19.0	−3.9 to −5.0
1991 Tubeworm Pillar area	10.2		−31.5		−3.7
1994–1997 Tubeworm Pillar area	0.21 to 0.38	0.10 to 0.12	−32.6 to −33.8	−21.0 to −22.5	−4.1 to −4.8

[a] From *Proskurowski et al.* [2008].

[31] Phase separation and segregation processes can decouple methane and manganese and cause variation their relative abundance. The high degree of variation in methane to Mn evident in Figures 2 and 5 is probably due to varying degrees of methane consumption in the plume, but also to variation in the methane to Mn in the source fluids. ^{3}He and methane are not expected to be closely coupled in source fluids because the ^{3}He has a magmatic source while the methane may be largely methanogenic or thermogenic. In addition, methane bearing near-bottom fluids, which have undergone varying degrees of methane consumption, could be entrained in the plume, further complicating the interpretation of these data. This probable variability in CH_4/Mn and CH_4/^{3}He in source fluids makes calculation of a fractionation factor for methane oxidation unreliable for this data set.

5.7. Methane Source Composition

[32] A reliable fraction remaining cannot be calculated; however, the samples with the highest concentrations of methane, Mn and ^{3}He can be assumed to have the composition closest to that of the source fluid(s). The δ^{13}C of the sample with the highest concentration of these parameters is −29.6‰ and most of the highest concentration samples in the upper plume have values close to this, while high-methane near-bottom samples are slightly more depleted (Data Set S1). The composition of these samples can be compared to known values for the isotopic composition of sources of methane in this system.

[33] The isotopic composition of methane in hydrothermal systems has been reviewed in numerous studies [e.g., *Kelley and Fruh-Green*, 1999; *Kelley et al.*, 2004; *Lilley et al.*, 1993; *Welhan*, 1988]. Given the wide range of values and the influence of site specific factors, we feel the most the most appropriate comparisons are to the stable isotopic carbon measurements of vent fluids and biota at this site. The methane in high-temperature vents is assumed to be primarily "high-temperature" methane as opposed to microbial or methanogenic. Between 1992 and 2000 high-temperature fluids at the EPR had a δ^{13}C of −20.1‰ ± 1.2‰, while those of diffuse fluids ranged from −25‰ to −34‰ between 1992 and 1997 [*Proskurowski et al.*, 2008] (Table 2). By contrast, high-temperature fluids in 1991 had δ^{13}C of −34‰ to −35‰, and thus resemble the lower temperature fluids. This may reflect the difficulty of sampling high-temperature fluid issuing directly from fissures in the basalt. *Proskurowski et al.* [2008] used a model to show that methane in low-temperature diffuse fluids at this site is controlled by a combination of mixing of high-temperature fluids, methanogenesis and microbial methane oxidation during the formation of diffuse fluids. Their model requires a low fractionation factor for methanogenesis, similar to what is expected at elevated temperatures [*Valentine et al.*, 2004]. Extrapolating the fractionation factors of *Valentine et al.* [2004] to this site, methane produced from a CO_2 substrate at −4‰ [*Proskurowski et al.*, 2008] could be as enriched as −27‰. This would extend the range for microbial methane composition considerably since microbially produced methane is usually thought to be −50‰ or more depleted [e.g., *Welhan*, 1988].

[34] Another possible source for this eruption-related methane may be thermogenic, i.e., methane produced by the breakdown of heated organic matter. Rapid pyrolysis of biomass has been shown to produce significant amounts of methane, though the details vary according the exact conditions, catalysis, and biomass material [*Yaman*, 2004]. The δ^{13}C of EPR mussels (foot, mantle, and adductor muscle tissue collected in April 2004), was between −31.55‰ and −33.41‰ versus PDB (T. M. Shank, unpublished data, 2004). At high temperatures and high reaction rates, little fractionation is expected in the production of methane from organic matter, while lower temperature and lower extent of reaction will produce methane that is depleted relative to the source carbon [*Tang et*

al., 2000]. Therefore, if mussels similar to those collected in 2004 were a carbon source for thermogenic production, the methane produced would be expected to have a composition at least as depleted as −31‰. However, the rapid cooling of the lava flow makes the continued production of methane by this process months after the eruption somewhat problematic. Methane is produced at temperatures as low as 125°C, but production increases with increased temperature [*Seewald et al.*, 1998]. It is possible that organic matter trapped beneath lava flows may become anoxic due both to organic matter oxidation and the low redox potential of volcanic rocks, resulting in continued methane production like that in sedimentary settings; however, this has never been documented. Eruption-related fluids could be stored in the crust and released over time but there is no established mechanism for this either, and it would probably result in further changes to the concentration and isotopic composition of the methane through microbial activity.

[35] Methanogenesis probably does play a role, as it has been observed in culture experiments of sulfide collected at this site [*Houghton et al.*, 2007], and thermogenesis is also likely, though the extent and duration are unknown. The measurements of δ^{13}C in this study cannot distinguish between methanogenic and thermogenic sources for methane because of the extremely high degree of overlap between the approximate ranges for microbially produced methane (−70‰ to −27‰) and for thermogenic methane (−50‰ to −31‰) discussed above.

6. Conclusions

[36] The water column signature in methane and manganese following the recent 2005/2006 eruptions on the EPR is similar to that observed after the 1991 eruption at the same site: methane and CH_4/Mn were elevated in the area most effected by the eruption, and the correlation between methane and Mn was relatively weak. However, the maximum observed methane concentration was 347 nM in the upper plumes, and as high as 1085 nM in near-bottom samples, exceeding concentrations observed in 1991. Manganese concentrations in 2005/2006, up to 55 nM in the upper plume samples and 98 nM in near-bottom samples, also exceeded the maximum of 18 nM observed in the eruption area in 1991. The CH_4/Mn ratio reached a maximum of 6.7, was greatest in the areas most affected by the eruption and is slightly lower on average than that observed in 1991. By contrast, maximum $CH_4/^3He$ ratios were very similar to those measured at this site in 1991 and at Axial volcano in 1998. The strikingly low Mn concentrations observed in 1991, in the area of the greatest methane concentrations (i.e., the immediate vicinity of the fresh flows), were not observed in 2006. Near-bottom samples collected with the TowCam show a significantly different chemical signature than the upper plume samples, probably due to the greater influence of low-temperature diffuse venting, the associated biological communities, the development of expansive areas of microbial mats, and the effects of large volumes of biomass buried by recently erupted lava flows. The influence methanogenesis versus thermogenesis cannot be distinguished due to the very similar range of isotopic compositions possible for production of methane by both processes. Some samples were extremely enriched in $^{13}CH_4$ due to microbial oxidation of plume methane, including a sample at +21‰, which is among the most isotopically enriched methane measured in a hydrothermal plume.

Acknowledgments

[37] We thank the captain and crew of R/V *New Horizon* and the marine operations personnel at Scripps Institution for organizing the logistics and ship operations of on such short notice. At NSF, L. Goad, R. Batiza, B. Haq, and A. Shor facilitated the scheduling and funding of this response cruise. Colleagues on the R/V *Knorr* (D. Forsyth and A. Saal, co-Ch. Sci.) made their key preliminary data available to us and helped us plan our surveys. D. Hebel, C. Khambatta, and E. Simms were instrumental in the collection of many of the samples. The Ridge2000 Office provided exceptional logistical support for this work. We acknowledge our reviewers for their thoughtful comments and suggestions. This field work was supported by NSF awards OCE0222069 (J.P.C., M.D.L.); OCE0525863 (D.J.F.); and OCE0327261 (T.M..S.); and the NASA Astrobiology Institute (JPC). The NOAA-VENTS program provided additional support through a grant to the Joint Institute for the Study of the Atmosphere and Ocean (JISAO) under NOAA Cooperative Agreement NA17RJ1232; JISAO contribution 1430; and PMEL contribution 3117 (J.A.R.). The manuscript was considerably improved by thoughtful reviews from R. Keir, W. Seyfried, V. Salters, and anonymous reviewers.

References

Baker, E. T., and H. B. Milburn (1997), MAPR: A new instrument for hydrothermal plume mapping, *RIDGE Events*, *8*, 23–25.

Baker, E. T., R. A. Feely, M. J. Mottl, F. T. Sansone, C. G. Wheat, J. A. Resing, and J. E. Lupton (1994), Hydrothermal plumes along the East Pacific Rise, 8°40′ to 11°50′N: Plume distribution and relationship to the apparent magmatic budget, *Earth Planet. Sci. Lett.*, *128*, 1–17, doi:10.1016/0012-821X(94)90022-1.

Carbotte, S., and K. Macdonald (1992), East Pacific Rise 8°–10°30′N: Evolution of ridge segments and discontinuities from SeaMARC II and three-dimensional magnetic studies, *J. Geophys. Res.*, *97*(B5), 6959–6982.

Charlou, J. L., H. Bougault, P. Appriou, P. Jeanbaptiste, J. Etoubleau, and A. Birolleau (1991), Water column anomalies associated with hydrothermal activity between 11°40′ and 13°N on the East Pacific Rise: Discrepancies between tracers, *Deep Sea Res., Part A*, *38*, 569–596, doi:10.1016/0198-0149(91)90064-M.

Coleman, D. D., J. B. Risatti, and M. Schoell (1981), Fractionation of carbon and hydrogen isotopes by methane-oxidizing bacteria, *Geochim. Cosmochim. Acta*, *45*, 1033–1037, doi:10.1016/0016-7037(81)90129-0.

Cowen, J. P., M. A. Bertram, E. T. Baker, R. A. Feely, G. J. Massoth, and M. Summit (1998), Geomicrobial transformation of manganese in Gorda Ridge event plumes, *Deep Sea Res., Part II*, *45*, 2713–2737, doi:10.1016/S0967-0645(98)00090-3.

Cowen, J. P., X. Y. Wen, and B. N. Popp (2002), Methane in aging hydrothermal plumes, *Geochim. Cosmochim. Acta*, *66*, 3563–3571, doi:10.1016/S0016-7037(02)00975-4.

Cowen, J. P., et al. (2007), Volcanic eruptions at East Pacific Rise near 9°50′N, *Eos Trans. AGU*, *88*, 81.

de Angelis, M. A., M. D. Lilley, E. J. Olson, and J. A. Baross (1993), Methane oxidation in deep-sea hydrothermal plumes of the Endeavour segment of the Juan-de-Fuca Ridge, *Deep Sea Res., Part I*, *40*, 1169–1186, doi:10.1016/0967-0637(93)90132-M.

Detrick, R. S., P. Buhl, E. E. Vera, J. C. Mutter, J. A. Orcutt, J. A. Madsen, and T. M. Brocher (1987), Multi-channel seismic imaging of a crustal magma chamber along the East Pacific Rise, *Nature*, *326*, 35–41, doi:10.1038/326035a0.

Escartín, J., S. A. Soule, D. J. Fornari, M. A. Tivey, H. Schouten, and M. R. Perfit (2007), Interplay between faults and lava flows in construction of the upper oceanic crust: The East Pacific Rise crest 9°25′–9°58′N, *Geochem. Geophys. Geosyst.*, *8*, Q06005, doi:10.1029/2006GC001399.

Ferrini, V. L., D. J. Fornari, T. M. Shank, J. C. Kinsey, M. A. Tivey, S. A. Soule, S. M. Carbotte, L. L. Whitcomb, D. Yoerger, and J. Howland (2007), Submeter bathymetric mapping of volcanic and hydrothermal features on the East Pacific Rise crest at 9°50′N, *Geochem. Geophys. Geosyst.*, *8*, Q01006, doi:10.1029/2006GC001333.

Fornari, D. J. (2003), A new deep-sea towed digital camera and multi-rock coring system, *Eos Trans. AGU*, *84*, 69, doi:10.1029/2003EO080001.

Fornari, D. J., R. M. Haymon, M. R. Perfit, T. K. P. Gregg, and M. H. Edwards (1998a), Axial summit trough of the east Pacific rise 9°–10°N: Geological characteristics and evolution of the axial zone on fast spreading mid-ocean ridges, *J. Geophys. Res.*, *103*, 9827–9855.

Fornari, D. J., T. Shank, K. L. Von Damm, T. K. P. Gregg, M. Lilley, G. Levai, A. Bray, R. M. Haymon, M. R. Perfit, and R. Lutz (1998b), Time-series temperature measurements at high-temperature hydrothermal vents, East Pacific Rise 9°49′–51′N: Evidence for monitoring a crustal cracking event, *Earth Planet. Sci. Lett.*, *160*, 419–431, doi:10.1016/S0012-821X(98)00101-0.

Fornari, D. J., et al. (2004), Submarine lava flow emplacement at the East Pacific Rise 9°50′N: Implications for uppermost ocean crust stratigraphy and hydrothermal fluid circulation, in *Mid-Ocean Ridges: Hydrothermal Interactions Between the Lithosphere and Oceans*, *Geophys. Monogr. Ser.*, vol. 148, edited by C. R. German, J. Lin, and L. M. Parson, pp. 187–218, AGU, Washington, D. C.

Gamo, T., U. Tsunogai, S. Ichibayashi, and A. Hirota (2003), "Microbial plumes" as inferred from the increase of stable carbon isotope composition of methane originated from submarine hydrothermal activity, *Geochim. Cosmochim. Acta*, *67*, A115.

Gharib, J. J., F. J. Sansone, J. A. Resing, E. T. Baker, J. E. Lupton, and G. J. Massoth (2005), Methane dynamics in hydrothermal plumes over a superfast spreading center: East Pacific Rise, 27.5°–32.3°S, *J. Geophys. Res.*, *110*, B10101, doi:10.1029/2004JB003531.

Haymon, R. M., et al. (1993), Volcanic eruption of the mid-ocean ridge along the East Pacific Rise crest at 9°45–52′N: Direct submersible observations of seafloor phenomena associated with an eruption event in April, 1991, *Earth Planet. Sci. Lett.*, *119*, 85–101, doi:10.1016/0012-821X(93)90008-W.

Houghton, J. L., W. E. Seyfried, A. B. Banta, and A. L. Reysenbach (2007), Continuous enrichment culturing of thermophiles under sulfate and nitrate-reducing conditions and at deep-sea hydrostatic pressures, *Extremophiles*, *11*, 371–382, doi:10.1007/s00792-006-0049-7.

Jackett, D. R., T. J. McDougall, R. Feistel, D. G. Wright, and S. M. Griffies (2006), Algorithms for density, potential temperature, conservative temperature, and the freezing temperature of seawater, *J. Atmos. Oceanic Technol.*, *23*, 1709–1728, doi:10.1175/JTECH1946.1.

Kadko, D. C., N. D. Rosenberg, J. E. Lupton, R. W. Collier, and M. D. Lilley (1990), Chemical reaction rates and entrainment within the Endeavor Ridge hydrothermal plume, *Earth Planet. Sci. Lett.*, *99*, 315–335, doi:10.1016/0012-821X(90)90137-M.

Kelley, D. S., and G. L. Fruh-Green (1999), Abiogenic methane in deep-seated mid-ocean ridge environments: Insights from stable isotope analyses, *J. Geophys. Res.*, *104*, 10,439–10,460.

Kelley, D. S., M. D. Lilley, J. E. Lupton, and E. J. Olson (1998), Enriched H_2, CH_4, and ^{3}He concentrations in hydrothermal plumes associated with the 1996 Gorda Ridge eruptive event, *Deep Sea Res., Part II*, *45*, 2665–2682, doi:10.1016/S0967-0645(98)00088-5.

Kelley, D. S., M. D. Lilley, and G. L. Fruh-Green (2004), Volatiles in submarine environments: Food for life, in *The Subseafloor Biosphere at Mid-Ocean Ridges*, *Geophys. Monogr. Ser.*, vol. 144, edited by W. S. D. Wilcock et al., pp. 167–189, AGU, Washington, D. C.

Kent, G. M., A. J. Harding, and J. A. Orcutt (1993), Distribution of magma beneath the East Pacific Rise between the Clipperton Transform and the 9°17′N Deval from forward modeling of common depth point data, *J. Geophys. Res.*, *98*, 13,945–13,969.

Langmuir, C. H., J. F. Bender, and R. Batiza (1986), Petrological and tectonic segmentation of the East Pacific Rise, 5°30′–14°30′N, *Nature*, *322*, 422–429, doi:10.1038/322422a0.

Lilley, M. D., E. Olson, E. McLaughlin, and K. L. Von Damm (1991), Methane, hydrogen and carbon dioxide in vent fluids from the 9°N hydrothermal system, *Eos Trans. AGU*, *72*(44), Fall Meet. Suppl., 481.

Lilley, M. D., D. A. Butterfield, E. J. Olson, J. E. Lupton, S. A. Macko, and R. E. McDuff (1993), Anomalous CH_4 and NH_4^+ concentrations at an unsedimented mid-ocean ridge hydrothermal system, *Nature*, *364*, 45–47, doi:10.1038/364045a0.

Lilley, M., R. A. Feely, and J. A. Trefry (1995), Chemical and biochemical transformations in hydrothermal plumes, in *Sea-*

floor Hydrothermal Systems: Physical, Chemical, Biological, and Geological Interactions, *Geophys. Monogr. Ser.*, vol. 91, edited by S. E. Humphris et al., pp. 369–391, AGU, Washington, D. C.

Lupton, J. E., E. T. Baker, M. J. Mottl, F. J. Sansone, C. G. Wheat, J. A. Resing, G. J. Massoth, C. I. Measures, and R. A. Feely (1993), Chemical and physical diversity of hydrothermal plumes along the East Pacific Rise, 8°45′N to 11°50′N, *Geophys. Res. Lett.*, *20*, 2913–2916, doi:10.1029/93GL00906.

Lutz, R. A., T. M. Shank, D. J. Fornari, R. M. Haymon, M. D. Lilley, K. L. Von Damm, and D. Desbruyeres (1994), Rapid growth at deep-sea vents, *Nature*, *371*, 663–664, doi:10.1038/371663a0.

Macdonald, K. C., et al. (1992), The East Pacific Rise and its flanks 8–18°N: History of segmentation, propagation and spreading direction based on SeaMARC II and Sea Beam studies, *Mar. Geophys. Res.*, *14*(4), 299–344.

McLaughlin-West, E. A., E. J. Olson, M. D. Lilley, J. A. Resing, J. E. Lupton, E. T. Baker, and J. P. Cowen (1999), Variations in hydrothermal methane and hydrogen concentrations following the 1998 eruption at Axial Volcano, *Geophys. Res. Lett.*, *26*, 3453–3456, doi:10.1029/1999GL002336.

Mottl, M. J., F. J. Sansone, C. G. Wheat, J. A. Resing, E. T. Baker, and J. E. Lupton (1995), Manganese and methane in hydrothermal plumes along the East Pacific Rise, 8°–40′ to 11°50′N, *Geochim. Cosmochim. Acta*, *59*, 4147–4165, doi:10.1016/0016-7037(95)00245-U.

Perfit, M. R., and W. W. Chadwick (1998), Magmatism at mid-ocean ridges: Constraints from volcanological and geochemical investigations, in *Faulting and Magmatism at Mid-Ocean Ridges*, *Geophys. Monogr. Ser.*, vol. 106, edited by W. R. Buck et al., pp. 59–116, AGU, Washington, D. C.

Perfit, M. R., D. J. Fornari, M. C. Smith, J. F. Bender, C. H. Langmuir, and R. M. Haymon (1994), Small-scale spatial and temporal variations in midocean ridge crest magmatic processes, *Geology*, *22*, 375–379, doi:10.1130/0091-7613(1994)022<0375:SSSATV>2.3.CO;2.

Popp, B. N., F. J. Sansone, T. M. Rust, and D. A. Merritt (1995), Determination of concentration and carbon isotopic composition of dissolved methane in sediments and near-shore waters, *Anal. Chem.*, *67*, 405–411, doi:10.1021/ac00098a028.

Proskurowski, G., M. D. Lilley, and E. J. Olson (2008), Stable isotopic evidence in support of active microbial methane cycling in low-temperature diffuse flow vents at 9°50′N East Pacific Rise, *Geochim. Cosmochim. Acta*, *72*(8), 2005–2023, doi:10.1016/j.gca.2008.01.025.

Rubin, K. H., J. D. Macdougall, and M. R. Perfit (1994), ^{210}Po-^{210}Pb dating of recent volcanic eruptions on the seafloor, *Nature*, *368*, 841–844, doi:10.1038/368841a0.

Rubin, K. H., M. R. Perfit, D. J. Fornari, S. A. Soule, and M. Tolstoy (2006), Geochronology and composition of the 2005–06 volcanic eruptions of the East Pacific Rise, 9°46′–56′N, *Eos Trans. AGU*, *87*(52), Fall Meet. Suppl., Abstract V23B-0602.

Sansone, F. J., B. N. Popp, and T. M. Rust (1997), Stable carbon isotopic analysis of low-level methane in water and gas, *Anal. Chem.*, *69*, 40–44, doi:10.1021/ac960241i.

Sansone, F. J., M. E. Holmes, and B. N. Popp (1999), Methane stable isotopic ratios and concentrations as indicators of methane dynamics in estuaries, *Global Biogeochem. Cycles*, *13*, 463–473, doi:10.1029/1999GB900012.

Scheirer, D. S., and K. C. Macdonald (1993), Variation in cross-sectional area of the axial ridge along the East Pacific Rise: Evidence for the magmatic budget of a fast spreading center, *J. Geophys. Res.*, *98*(B5), 7871–7885.

Seewald, J. S., B. C. Benitez-Nelson, and J. K. Whelan (1998), Laboratory and theoretical constraints on the generation and composition of natural gas, *Geochim. Cosmochim. Acta*, *62*, 1599–1617, doi:10.1016/S0016-7037(98)00000-3.

Shank, T. M., D. J. Fornari, K. L. Von Damm, M. D. Lilley, R. M. Haymon, and R. A. Lutz (1998), Temporal and spatial patterns of biological community development at nascent deep-sea hydrothermal vents (9°50′N, East Pacific Rise), *Deep Sea Res., Part II*, *45*, 465–515.

Silverman, M. P., and V. I. Oyama (1968), Automatic apparatus for sampling and preparing gases for mass spectral analysis in studies of carbon isotope fractionation during methane metabolism, *Anal. Chem.*, *40*, 1833–1837, doi:10.1021/ac60268a001.

Soule, S. A., D. J. Fornari, M. R. Perfit, and K. H. Rubin (2007), New constraints on mid-ocean ridge eruption processes from the 2005–06 eruption of the East Pacific Rise, 9°46′–9°56′N, *Geology*, *35*, 1079–1082, doi:10.1130/G23924A.1.

Tang, Y., J. K. Perry, P. D. Jenden, and M. Schoell (2000), Mathematical modeling of stable carbon isotope ratios in natural gases, *Geochim. Cosmochim. Acta*, *64*, 2673–2687, doi:10.1016/S0016-7037(00)00377-X.

Tolstoy, M., et al. (2006), A sea-floor spreading event captured by seismometers, *Science*, *314*, 1920–1922, doi:10.1126/science.1133950.

Tolstoy, M., F. Waldhauser, D. R. Bohnenstiehl, R. T. Weekly, and W. Y. Kim (2008), Seismic identification of along-axis hydrothermal flow on the East Pacific Rise, *Nature*, *451*, 181–187, doi:10.1038/nature06424.

Valentine, D. L., A. Chidthaisong, A. Rice, W. S. Reeburgh, and S. C. Tyler (2004), Carbon and hydrogen isotope fractionation by moderately thermophilic methanogens, *Geochim. Cosmochim. Acta*, *68*, 1571–1590, doi:10.1016/j.gca.2003.10.012.

Von Damm, K. L. (2000), Chemistry of hydrothermal vent fluids from 9°–10°N, East Pacific Rise: "Time zero," the immediate posteruptive period, *J. Geophys. Res.*, *105*, 11,203–11,222.

Von Damm, K. L., and M. Lilley (2004), Diffuse flow hydrothermal fluids from 9°50′N East Pacific Rise: Origin, evolution and biogeochemical controls, in *The Subseafloor Biosphere at Mid-Ocean Ridges*, *Geophys. Monogr. Ser.*, vol. 144, edited by W. S. D. Wilcock et al., pp. 245–268, AGU, Washington, D. C.

Von Damm, K. L., S. E. Oosting, R. Kozlowski, L. G. Buttermore, D. C. Colodner, H. N. Edmonds, J. M. Edmond, and J. M. Grebmeier (1995), Evolution of East Pacific Rise hydrothermal vent fluids following a volcanic eruption, *Nature*, *375*, 47–50, doi:10.1038/375047a0.

Welhan, J. A. (1988), Origin of methane in hydrothermal systems*Chem. Geol.*, *71*, 183–198, doi:10.1016/0009-2541(88)90114-3.

White, S. M., R. M. Haymon, and S. Carbotte (2006), A new view of ridge segmentation and near-axis volcanism at the East Pacific Rise, 8°–12°N, from EM300 multibeam bathymetry, *Geochem. Geophys. Geosyst.*, *7*, Q12O05, doi:10.1029/2006GC001407.

Yaman, S. (2004), Pyrolysis of biomass to produce fuels and chemical feedstocks, *Energy Convers. Manage.*, *45*, 651–671, doi:10.1016/S0196-8904(03)00177-8.